Origin of the spontaneous orientational ordering of islands during thin film growth

Jikeun Seo[1] and Jae-Sung Kim[2]
[1]*Department of Ophthalmic Optics, Chodang University, Muan 58530, Korea*
[2]*Department of Physics, Sook-Myung Women's University, Seoul 04310, Korea*
(Received 3 February 2016; revised manuscript received 23 May 2017; published 1 August 2017)

The spontaneous orientational order of some metal islands on Cu(001) along ⟨100⟩ has long eluded its explanation, which is now revealed by the study with the kinetic Monte Carlo simulation. The orientational order originates from the relative stability of the diagonal orientation of the neighboring islands against their coalescence. That stability results from the square symmetry of the islands, since the diagonally meeting islands have the minimum contact area mediating their merge. Moreover, we well reproduce and elucidate the orientational order propagating into the following several tens of monolayers. The orientational order of the islands is driven simply by the symmetry of the surface unit cell and is thus generic in the epitaxial growth, making pervasive effects on the physical properties of the epitaxial films.

DOI: 10.1103/PhysRevB.96.085402

I. INTRODUCTION

Thin film growth by vapor deposition typically proceeds via the adsorption of the evaporants followed by nucleation and growth of the immobile clusters and then their coalescence [1–3]. Incident flux distribution is usually assumed homogeneous, and the nucleation of the clusters is mediated by random diffusion and adhesion of the adatoms. According to this picture, the islands are expected to be distributed over the substrate with no preferred orientation among them.

Some aspects of that standard picture, although they look very natural, have proven wrong. For example, the deposition flux is found not uniform, because the incident atom interacts with the substrate and the islands already on it and is steered towards the islands [4–10]. The inhomogeneous deposition flux makes the film rougher [4,6], drives the instability during its growth [11], and alters the symmetry of the islands from that of the substrate [4,5,7,8]. The deposition dynamics offers useful parameters to manipulate the physical properties of the thin films, e.g., the shape anisotropy of the magnetic films grown by deposition at oblique angles [12].

Another anomaly to the standard picture is very intriguing; Bartelt and Evans observed the fourfold lobes in the Henzler ring in their growth simulation on fcc (001) and suggested it to originate from the depletion of the nearby pairs of islands [13]. Nyberg *et al.* [14] observed the fourfold lobes in the Henzler ring along ⟨100⟩ directions during the growth of Fe, Co, and Cu on Cu(001) by spot-profile analysis of low energy electron diffraction (SPA-LEED) and attributed them to the Fraunhofer diffraction of the square shaped islands. Later, Jorritsma *et al.* [15] also observed the fourfold robes during the growth of Cu on Cu(001), but the order was attributed to the orientational order of the islands. They suggest the preferential coalescence along ⟨100⟩ directions as the mechanism for the development of the order, since the growth speed of the adatom island is fastest in the diagonal direction. Durukanoğlu *et al.* [16] pointed to the lower step crossing barrier along ⟨100⟩ on Cu(001) than that along ⟨110⟩ as a possible origin of the orientational order. However, both do not address how the anisotropic aspects in the growth of the islands lead to the orientational order among the islands. That unexpected observation was reported more than two decades ago [14], but its origin still remains elusive, reflecting the intricate nature of the problem.

In this paper, we report the origin of the spontaneous orientational ordering of the islands that is disclosed by extensive kinetic Monte Carlo simulation (kMC). The fourfold lobes in the Henzler ring are assured to reflect the diagonally aligned islands and originate from the relative stability of the diagonal orientation of the neighboring islands against their coalescence. Each island repeats the coalescence with the neighboring islands until the island meets a neighboring island in the diagonal direction. The stability originates from the square symmetry of the island, because the diagonally meeting islands have the minimum contact area mediating their coalescence. With the increase of the coverage and the size of the island, the coalescence occurs frequently and globally, which facilitates the diagonal ordering of the islands.

With the further deposition, the islands interconnected by the coalescence simply grow via the lateral growth perpendicular to their edges. Since the lateral growth speed of diagonally meeting islands is maximal, the orientational order along the diagonal direction further improves as the coverage increases. Moreover, the orientational order is found to propagate to the overlayer via the guided nucleation and growth of the islands over the underlying islands, replicating the underlayer and its order in the following several tens of layers well reproducing the previous experimental observation [15].

II. SIMULATION SCHEME

kMC simulation is utilized to study the thin film growth by thermal deposition [7,8]. Deposition of Cu atoms on Cu(001) is assumed random, and its rate was 0.25 ML/min. Even when the deposition dynamics is taken into account, the ordering kinetics does not change. In the simulation, only the diffusion into empty fcc lattice sites is allowed and the exchange diffusion is not allowed. Also, the overhang sites are not allowed during both deposition and diffusion processes. The simulated system is composed of 400×400 square lattice mimicking fcc (001).

We used 32 different diffusion barriers corresponding to the 2^5 configurations determined by the existence or absence of

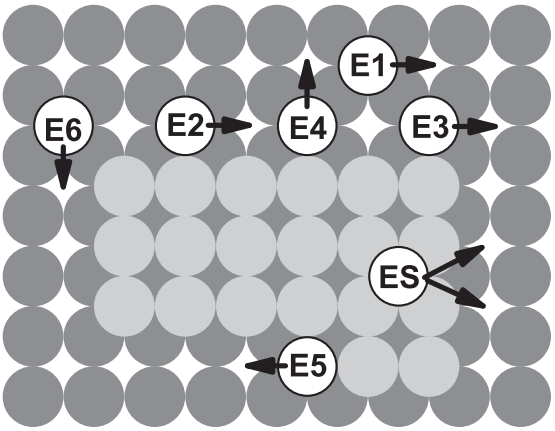

FIG. 1. Illustration of some of the important diffusion processes.

the atoms in the five nearest and the next nearest sites around a moving atom [11]. Values of the barriers are adopted from those of Furman and coworkers [17,18]. In addition to those barriers, five barriers accompanying Ehrlich-Schwoebel(ES) barrier are considered. The step ES barrier is 0.07 eV and the kink ES barrier is 0.035 eV. Some of the important diffusion processes are illustrated in Fig. 1, and their associated barrier energies are listed in Table I.

Note that the barrier for the diffusion along step edge (E2) is taken to be 0.40 eV in the present simulation, which is much larger than the real one, 0.20 eV in order to save the computation time. The use of this large E2, however, was found not to affect the morphology of the resulting films [7,8].

III. RESULTS AND DISCUSSION

Figure 2(a) shows a snapshot after depositing 0.4 ML of Cu on Cu(001), normal to the surface at 250 K. Figure 2(a′) is the Fourier transformed image from 400 snapshots obtained by the simulations iterated under the same growth condition. The Henzler ring in Fig. 2(a′) shows no distinguished peak around its circumference, telling that little anisotropic feature has developed on the surface.

With slightly increased coverage of 0.75 ML [Fig. 2(b)], contrastingly, well-defined fourfold symmetric peaks develop in the Henzler ring along ⟨100⟩ directions as shown in

TABLE I. Diffusion barriers and parameters adopted in our simulation.

Type of diffusion	Diffusion barrier
E1	0.42 eV
E2	0.40 eV
E3	0.48 eV
E4	0.68 eV
E5	0.40 eV
E6	0.18 eV
ES barrier (ES)	0.07 eV (0.42 + 0.07 eV)
ES barrier (kink site)	0.035 eV
jump frequency (ν_0)	3.6×10^{12}
deposition rate (F_0)	0.25 ML/min

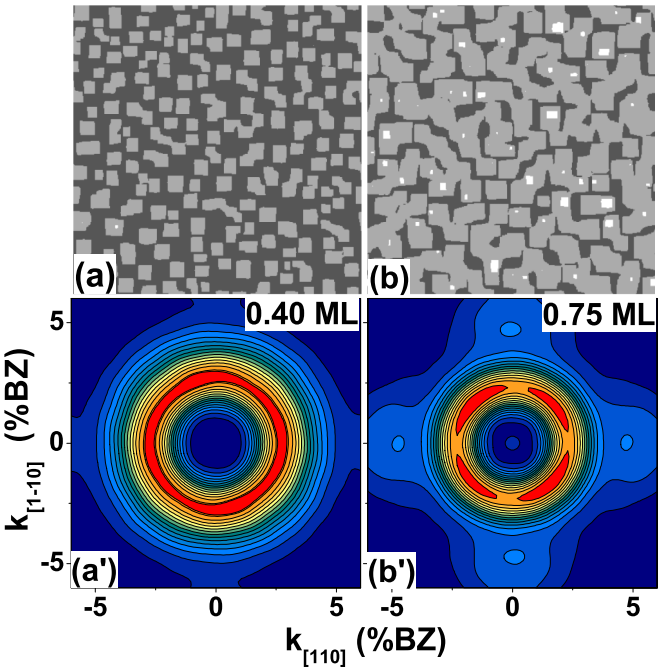

FIG. 2. Illustration of the initial stage of thin film growth and the development of order. Representative simulated images, respectively, after depositing (a) 0.4 ML and (b) 0.75 ML of Cu on Cu(001), normal to the surface at 250 K. Each image shows 400 × 400 atomic lattice. (a′) [(b′)] is the Fourier transformed image from 400 images of 0.4 (0.75) ML Cu on Cu(001).

Fig. 2(b′). The present simulation reproduces the previous experimental observation of Nyberg *et al.* [14] and Jorritsma *et al.* [15] by SPA-LEED. The two groups, though, suggested different origins for the peaks in the Henzler ring: Fraunhoffer diffraction of the islands by the former and the orientational ordering of the Cu islands by the latter.

In order to identify the origin of the peaks, we regularly arrange both the square and rhombus islands along ⟨100⟩ directions, as shown, respectively, in Figs. 3(a) and 3(b), and then randomly perturb their positions within ±25 a_o along ⟨110⟩ directions. a_o is the surface lattice constant or the nearest neighbor distance on Cu(001). Their Fourier transformed images in Figs. 3(a′) and 3(b′) commonly show the peaks in the Henzler ring along the ⟨100⟩ directions, irrespective of the shape of the islands. If the square islands are similarly arranged, but along ⟨110⟩ directions and perturbed as shown in Fig. 3(c), then the peaks in the Henzler ring now appear along ⟨110⟩ directions in Fig. 3(c′). Those observations consistently tell that the peaks in the Henzler ring originate from the orientational order of the islands.

The Fraunhoffer diffraction pattern of the islands indeed develops. Relatively weak, but well-defined fourfold symmetric features are observed outside the central peak along ⟨110⟩ (⟨100⟩) directions in Figs. 3(a′) and 3(c′) (Fig. 3(b′)), reflecting the symmetry of the islands.

As a measure of the orientational order of the islands, we take the ratio η of the diffraction intensity in the Henzler ring along the ⟨100⟩ direction $I_{\langle 100\rangle}$ to that along ⟨110⟩, $I_{\langle 110\rangle}$ and present it as a function of the coverage θ in Fig. 4. If no orientational order of the islands develops, then η should

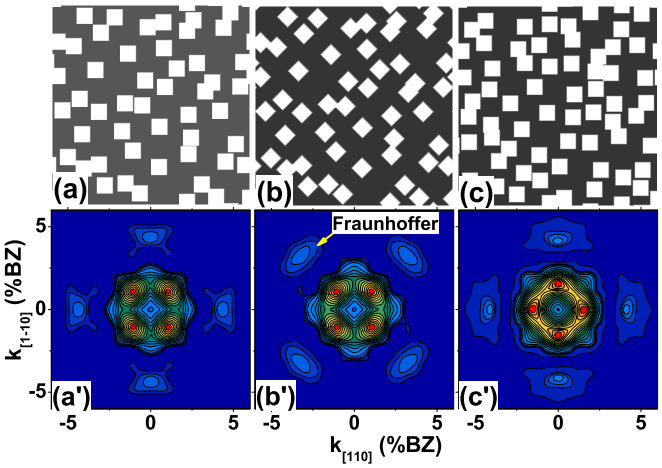

FIG. 3. (a) [(b)] A snapshot of perfectly diagonally ordered square (rhombus) islands, which are then laterally perturbed by ±25 a_o. a_o is the surface lattice constant or the distance to the nearest neighbor. (a′) [(b′)] Fourier transformed image from the 400 snapshots like (a) [(b)]. (c) A snapshot of perfectly ordered square islands along ⟨110⟩ after lateral perturbation by ±25 a_o. (c′) Fourier transformed image from the 400 snapshots like (c).

be 1. For $\theta <\sim 0.55$ ML, η is smaller than 1. Fraunhoffer diffraction of the square islands form a broad peak outside the Henzler ring along ⟨110⟩ [see Fig. 2(b′)] and contribute to $I_{\langle 110\rangle}$, making $\eta < 1$, before there develops order along the ⟨100⟩ direction. η shows a minimum around 0.45 ML, indicating that the orientational order of the islands along ⟨100⟩ gradually builds up and competes with that from the Fraunhoffer diffraction. For $\theta >\sim 0.45$ ML, η monotonically increases and becomes larger than 1 for $\theta >\sim 0.55$ ML. The fourfold lobes gradually become discernible in the Henzler ring along ⟨100⟩. Accordingly, Jorritsma *et al.* [15] could experimentally observe the well-defined anisotropic intensity in the Henzler ring around $\theta \sim 0.7$ ML.

From Fig. 4, we notice that the orientational order of the islands develops in two distinct steps. In the first step or for $\theta <\sim 0.6$ ML, the growth rate of η monotonically increases with the increase of θ. In the second step or for $\theta >\sim 0.6$ ML, η grows with almost constant slope with respect to θ. We find that the orientational order has distinct origins in the two growth steps as detailed below.

The coverage at which the first step is completed shows the minimum in the rate of the island density change or the maximal rate of the coalescence of the islands as shown in the inset (a) of Fig. 4. We name this coverage as $\theta_p \sim 0.6$ ML. For $\theta > \theta_p$, the rate of the coalescence rapidly decreases as noted in the inset. This observation hints that the orientational order of the islands is related to the coalescence of the islands, or develops during the coalescence of the islands, as also suggested by Jorritsma *et al.* [15].

In order to disclose how the coalescence of the islands develops the orientational order in the first step, we examine the behavior of two adjacent islands under continued deposition. In Fig. 5(a), three pairs of two adjacent islands (red squares) are placed with their center-to-center orientation making angle

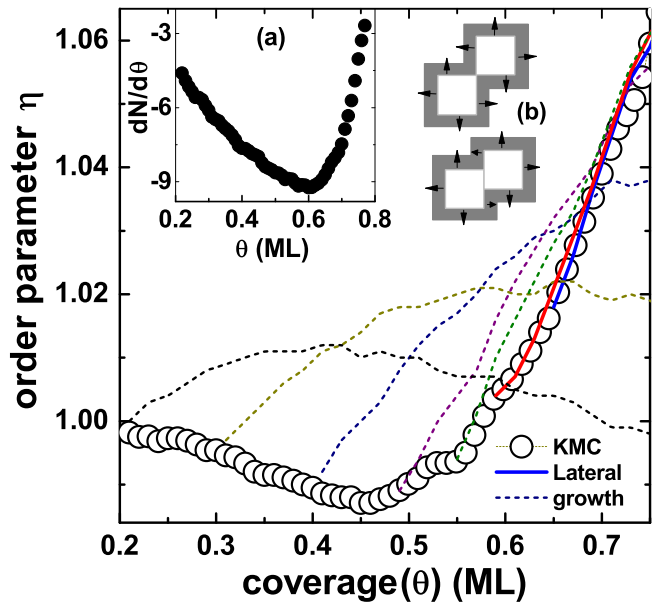

FIG. 4. η from the kMC simulation is plotted as a function of the coverage θ. Each dashed (solid) line signifies the evolution of $\eta(\theta)$ for $\theta > \theta_s$ by the lateral growth for different $\theta_s < \theta_p$ ($> \theta_p$). Insets : (a) The rate of the island density change as a function of θ. (b) Illustration of the lateral growth perpendicular to each edge of the island with the same growth speed.

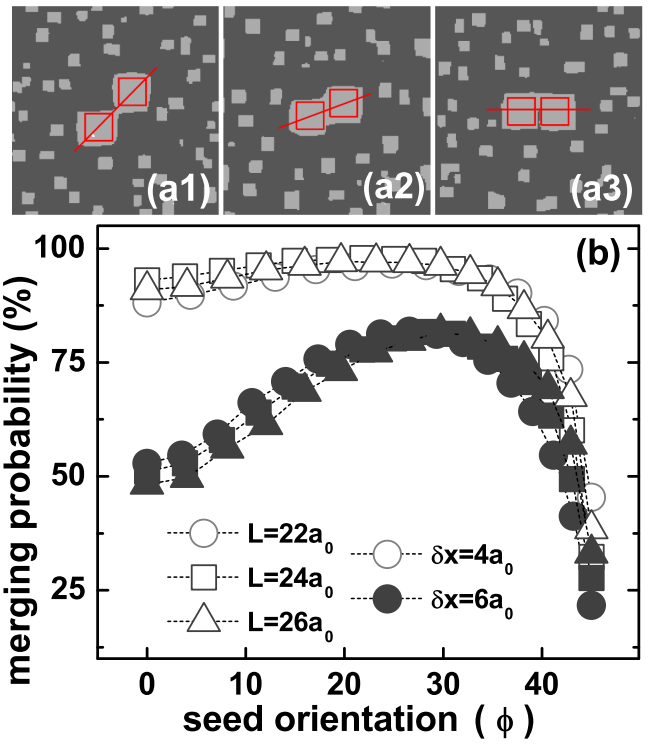

FIG. 5. (a1)–(a3) Three different pairs of adjacent islands (in red) with different center-to-center orientation making angle ϕs with respect to the x axis. Over the substrate with the pair of the islands, 0.15 ML is deposited to find their coalescence probability. (b) Coalescence probability of two adjacent islands under continued deposition as a function of ϕ. The plots are made, varying the initial edge length L and the initial separation of the two islands δx.

ϕs with respect to the x axis such that tanϕs are (a1) 1, (a2) 0.5, and (a3) 0. The size of the seed islands is chosen to be about the mean island size observed in our simulation after depositing 0.5 ML at 250 K, $L = 22 \sim 26$ a$_o$. Then, we study their behaviors after additionally depositing 0.15 ML over the surface.

Varying ϕ, L, and the initial separation of the two islands along the x axis δx, we repeat the simulation 16 000 times for each case. From the simulated images, we obtain the probability for the two islands to coalesce as summarized in Fig. 5(b). Note that the coalescence probability is minimum for tan$\phi = 1$ or $\phi = 45^\circ$ in Fig. 5(b), irrespective of the initial configuration of the seed islands. The coalescence probability increases rapidly, if the orientation of the two islands deviates from the diagonal direction. This tells that two islands are relatively stable against the coalescence when they meet diagonally, compared with the cases where they meet in the other orientations.

Once two islands are coalesced, the resulting island is left with arbitrary orientational relation with their neighboring islands [19]. During the growth of an island, thus, it would repeat the coalescence until it meets its neighboring island in the diagonal direction. Thereof, the diagonal orientation is selected during the growth of the islands. Approaching θ_p, this coalescence process occurs most frequently as shown in the inset (a) in Fig. 4, expediting the selection of the diagonally oriented islands.

The stability of the diagonal orientation of two adjacent islands against their coalescence originates from the symmetry of the square islands. If two islands are diagonally oriented as shown in Fig. 5(a1), then their coalescence proceeds through the restricted area around the corner region during their growth, and the coalescence probability remains low. If they are oriented in the off-diagonal directions as shown in Figs. 5(a2) and 5(a3), they would meet via the neighboring two edges during their growth; As two islands are oriented further away from the diagonal direction, the length of the neighboring edges increases, and so does the merging probability as shown in Fig. 5(b). However, if the neighboring edge length is too long as shown in Fig. 5(a3), the gap made by the two neighboring edges is inaccessible to the adatoms away from it. Then, the supply of the adatoms and so the growth of the two neighboring edges are limited, and the merging probability decreases as shown in Fig. 5(b).

We have further examined the case where the square islands have edges along ⟨100⟩ rather than along ⟨110⟩ by lowering E4 to 0.542 eV from 0.680 eV, while keeping all the other simulation parameters the same. Then, the peaks in the Henzler ring appear along ⟨110⟩, the diagonal directions of the islands, which is consistent with our picture [22]. The orientational ordering is observed for wide temperature range from 150 K and at least up to 310 K, the maximum simulated temperature that is limited only by the computational resources [22]. The spontaneous orientational order of the islands is, thus, sure to be a robust feature dictated by the symmetry of the islands.

In line with this picture, both Fe and Cu films on Cu(001) showed the pronounced orientational order along the diagonal direction. In contrast, the Co film on Cu(001) showed relatively weak anisotropy in the intensity of the Henzler ring [14], since Co islands have less propensity to form the square islands due to its hcp crystalline structure and the interface alloying [23,24] than Fe and Cu.

For $\theta > \theta_p$ or in the second step, most of the islands reside in a solid matrix of the interconnected islands, and the coalescence of the islands is not the major process during the continued deposition. This is also noted in the inset (a) of Fig. 4 that the magnitude of the island density change rapidly decreases for $\theta > \theta_p$. Instead, the lateral growth of the islands in the matrix determines the topographic evolution. We examine this conjecture by simulating this lateral growth as follows. We stop the kMC simulation at a certain coverage θ_s. For $\theta > \theta_s$, we laterally expand the islands by allowing equal growth speed perpendicular to every edge, as shown in the inset (b) of Fig. 4.

Figure 4 summarizes $\eta(\theta)$ for different θ_s along with that for the full kMC simulation. For $\theta_s > \theta_p$, to our surprise, $\eta(\theta)$ (solid lines) is almost coincidental with that for the full kMC simulation in sharp contrast to the case for $\theta_s < \theta_p$ (dashed lines). This observation tells that (1) the lateral growth indeed governs the surface topography for $\theta > \theta_p$, and (2) the distinction between the two steps comes from the different growth mechanisms of the islands. For $\theta_s < \theta_p$, the coalescence of islands as well as the lateral growth also plays a significant role, and $\eta(\theta)$ is not properly reproduced only by the lateral growth picture as shown in Fig. 4.

The reason why the lateral growth enhances the orientational order comes from the following two facts: Firstly, η is proportional to the area of the ordered island relative to the total area of the islands. [See Fig. 6(c) and the comment there.] Secondly, the diagonally meeting islands have the longer edge length per island and thus the larger speed of the areal growth

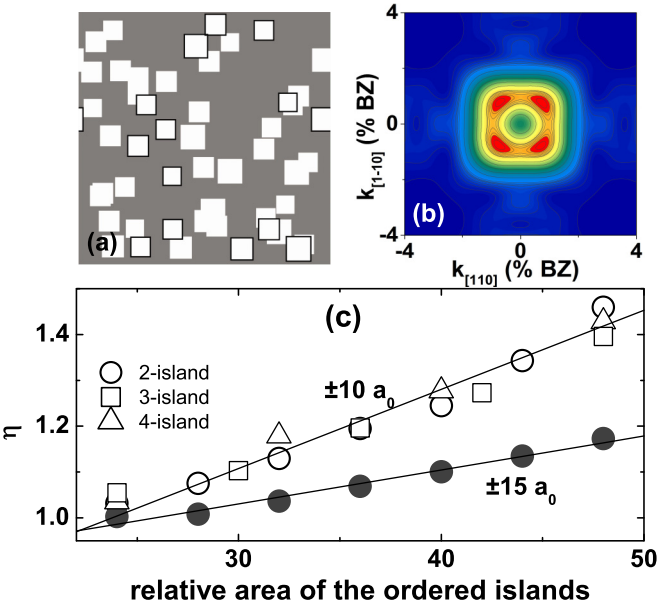

FIG. 6. (a) Chains of the two islands along ⟨100⟩ (in red) with the background islands (in white) forming the Henzler ring. Image size: 400 × 400 lattice. (b) Fourier transformed image of (a). (c) η is proportional to the area of the ordered islands relative to the total area of the islands. The islands in each chain are laterally perturbed by 10 (solid circle) and 15 (open circle) a$_o$ for comparison.

per island than the islands meeting off diagonally as noted in the inset (b) of Fig. 4.

According to the aforementioned picture, the orientational order of the islands develops via the repeated coalescence of the islands in the first step and thus could be kinetically limited. The question is, then, how long range the order of the islands should be to produce the observed anisotropic intensity around the Henzler ring. In order to answer this question, we construct the surface corresponding to 0.75 ML coverage as shown in Fig. 6(a) by randomly placing linear chains of two square islands along ⟨100⟩ that are depicted in red, along with the isotropically distributed islands (background islands) on 400×400 square lattice [Fig. 6(a)]. Since the ordered islands in each chain are not exactly aligned along ⟨100⟩, the center positions of the islands in each chain are randomly perturbed by ± 15 a_o for the best reproduction of the simulated image. In order for the background islands to have the short range order giving the Henzler ring, they are initially placed in the checker board pattern and then randomly disturbed by ± 50 a_o such that any anisotropic feature is not observed in the Henzler ring. The size of the islands is chosen to be the mean island size observed in our kMC simulation for 0.75 ML.

Figure 6(b) shows the Fourier transformed image of Fig. 6(a). Note that the intensity around the Henzler ring shows higher intensity along ⟨100⟩ than along any other direction. η is around 1.05 as observed in the kMC simulation for the same coverage [Fig. 4(b)]. From this construction, we find that the fourfold lobes in the Henzler ring can arise by only two-island-long order. Thus, the kinetic limitation associated with the coalescence of the islands does not deter the formation of the anisotropic intensity around the Henzler ring.

In Fig. 6(c), η is found to increase in proportion to the area of the aligned islands relative to the area of all the islands. For the larger lateral perturbation δx, η is the smaller as expected. Moreover, η is about the same, as far as the relative area of the aligned islands are the same, irrespective of the number of the constituent islands in each ordered chain; six two-island-long chains, four three-island-long chains, and three four-island-long chains, where each constituent island has the same area, give about the same η under otherwise the same condition [Fig. 6(c)]. This observation is not fully understood yet. Still, one thing clear is that the anisotropic intensity in the Henzler ring is produced mainly by the correlation between the adjacent islands, assuring the observation that the two-island-long order suffices to produce the anisotropic intensity in the Henzler ring.

Jorritsma *et al.* [15] also reported that the orientational order of the islands propagated with the continued growth of several tens of layers. In our simulation, the peaks in the Henzler ring are also observed up to the maximal simulated coverage 65 ML (Fig. 7). Layer resolved η in Fig. 7(a) tells that the maximal order η_{max} is observed within the five layers below the layer corresponding to the nominal coverage.

This persistent order is explained by the fact that the diagonally aligned islands are reproduced during the growth of the overlayer, and thus the orientational order of the underlayer is transferred to the overlayer. [See the inset of Fig. 7(b).] This peculiar growth is rationalized as follows: The orientational order in a layer is attributed to the islands diagonally meeting

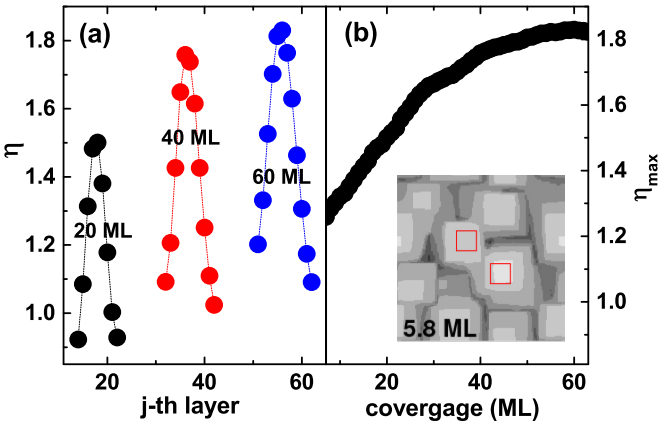

FIG. 7. (a) Layer resolved η for the coverages θs of 20, 40, and 60 MLs. The maximal order η_{max} is observed within the five layers below the layer corresponding to the coverage. (b) Plot of η_{max} as a function of θ. Inset: The seed island in the first layer (in red) is reproduced by the following layers.

through their corners. Then, the adatoms on an ordered island are isolated from those on the neighboring diagonally meeting island, because the transport of the adatoms between the surfaces of the two islands are restricted by the constriction at their corners. Then, the ad-island forms almost independently on each ordered island, replicating it in the overlayer.

Moreover, Fig. 7(b) shows that η_{max} monotonically increases to a saturation value $\sim$1.8 with the increase of the coverage. This indicates that the ordering of the islands proceeds in the growing layers via the continued coalescence of the nondiagonally oriented islands.

We end the discussion by assessing the previously proposed models for the origin of the anisotropic Henzler ring. Firstly, Bartelt *et al.* [13] suggested the depletion of the nearby pairs of islands as the origin of the anisotropic Henzler ring. If this picture is translated as the ordering of the vacancy islands after the percolation threshold, it is, then, consistent with our picture. Still, they did not address on the origin of the depletion of the islands. The Fraunhoffer diffraction of the islands [14] has proven not to produce the anisotropic Henzler ring as detailed in the discussion of Fig. 3.

Jorritsma *et al.* [15] advanced the anisotropic growth speed of the square island as the origin. The dotted lines in Fig. 4 show η after the lateral growth of the islands starts. The anisotropic growth speed during the lateral growth actually causes the anisotropic Henzler ring as judged by the growing η above 1. However, the dotted lines starting in the coverage where the coalescence of the islands is not frequent, *ca.*, less than 0.5 ML do not reproduce the kMC-simulated η, and is also contradictory to the experimental observation of the absence of the anisotropic Henzler ring for the coverage less than 0.7 ML. Hence, the observed anisotropic Henzler ring is not attributed to the anisotropic growth speed of the square islands.

Durukanoğlu *et al.* [16] pointed to the difference in the diffusion barrier over the step edges, ⟨100⟩ and ⟨110⟩ as the possible origin. We made the kMC simulation with the same diffusion barrier over the step edges along the two directions

and still observe the same anisotropy in the Henzler ring (figure not shown). The suggested mechanism is, thus, discarded.

IV. SUMMARY AND CONCLUSION

The extensive kMC simulation reveals that the spontaneous orientational order of the Cu islands on Cu(001) originates from the stability of the diagonal orientation of the neighboring islands against their coalescence. The islands meeting in the off-diagonal direction repeat merging until they meet one in the diagonal direction, which thus leads to the selection of the orientation of the neighboring islands along the diagonal direction. The stability of the diagonal orientation originates from the square symmetry of the island; the diagonally meeting islands have the minimum contact area mediating the formation of a merged island.

The orientational order propagates to the following layers via the replication of the ordered islands in the underlayer. Actually, the order improves with the increase of the coverage by the continued self-selection of the diagonal orientation of the islands in the growing layers.

The spontaneous orientational order of the islands is generic in thin film growth, since it is driven simply by the symmetry of surface unit cell. Its effects could be far reaching in the heteroepitaxial growth. For example, when Fe is grown on square symmetric substrates such as GaAs(001), the unintended ordering of Fe islands along the diagonal direction would give rise to anisotropic dipole-dipole interaction, which could be the source of the controversial in-plane magnetic anisotropy of the Fe film [25–27].

ACKNOWLEDGMENTS

We appreciate J. W. Evans for his detailed comments and suggestions. This work is supported by NRF - Contracts No. 2016M2B2A4912062 and No. 2016R1D1A1B03930532.

[1] H. Brune, Surf. Sci. Rep. **31**, 125 (1998).
[2] *The Chemical Physics of Solid Surfaces*, edited by D. A. King and D. P. Woodruff (Elsevier, Amsterdam, 1997), Vol. 8; *Morphological Organization in Expitaxial Growth and Removal*, edited by Z. Zhang and M. G. Lagally (World Scientific, Singapore, 1998).
[3] J. W. Evans, P. A. Thiel, and M. C. Bartelt, Suf. Sci. Rep. **61**, 1 (2006).
[4] S. v. Dijken, L. C. Jorritsma, and B. Poelsema, Phys. Rev. Lett. **82**, 4038 (1999).
[5] S. v. Dijken, L. C. Jorritsma, and B. Poelsema, Phys. Rev. B **61**, 14047 (2000).
[6] F. Montalenti and A. F. Voter, Phys. Rev. B **64**, 081401 (2001).
[7] J. Seo, S.-M. Kwon, H.-Y. Kim, and J.-S. Kim, Phys. Rev. B **67**, 121402 (2003).
[8] J. Seo, H.-Y. Kim, and J.-S. Kim, Phys. Rev. B **71**, 075414 (2005).
[9] J. Yu and J. G. Amar, Phys. Rev. Lett. **89**, 286103 (2002).
[10] Y. Shim and J. G. Amar, Phys. Rev. Lett. **98**, 046103 (2007).
[11] J. Seo, H.-Y. Kim, and J.-S. Kim, J. Phys.: Condens. Matter **19**, 486001 (2007).
[12] S. van Dijken, G. Di Santo, and B. Poelsema, Phys. Rev. B **63**, 104431 (2001).
[13] M. C. Bartelt and J. W. Evans, Surf. Sci. **298**, 421 (1993).
[14] G. L. Nyberg, M. T. Kief, and W. F. Eglehof, Jr., Phys. Rev. B **48**, 14509 (1993).
[15] L. C. Jorritsma, M. Bijnagte, G. Rosenfeld, and B. Poelsema, Phys. Rev. Lett. **78**, 911 (1997).
[16] S. Durukanoğlu, O. S. Trushin, and T. S. Rahman, Phys. Rev. B **73**, 125426 (2006).
[17] I. Furman, O. Biham, J.-K. Zuo, A. K. Swan, and J. F. Wendelken, Phys. Rev. B **62**, R10649(R) (2000).
[18] H. Mehl, O. Biham, I. Furman, and M. Karimi, Phys. Rev. B **60**, 2106 (1999).
[19] The *post-deposition* sintering of two coalesced islands into a square island requests a long time to overcome the various kink Ehrich-Schwoebel barriers [20]. However, in our simulation, most islands have the shapes similar to the square, which can be attributed to the growth dynamics involving nonequilibrium shape caused by the continued deposition [21].
[20] C. R. Stoldt, A. M. Cadilhe, C. J. Jenks, J.-M. Wen, J. W. Evans, and P. A. Thiel, Phys. Rev. Lett. **81**, 2950 (1998); D.-J. Liu and J. W. Evans, Phys. Rev. B **66**, 165407 (2002).
[21] J. W. Evans (private communication).
[22] See Supplemental Material at http://link.aps.org/supplemental/10.1103/PhysRevB.96.085402 for the detailed description of the island orientation dependence and temperature dependence.
[23] A. K. Schmidt and J. Kirchner, Ultramicroscopy. **42-44**, 483 (1992).
[24] O. Mironets, H. L. Meyerheim, C. Tusche, V. S. Stepanyuk, E. Soyka, H. Hong, P. Zschack, N. Jeutter, R. Felici, and J. Kirschner, Phys. Rev. B **79**, 035406 (2009).
[25] F. Bensch, R. Moosbühler, and G. Bayreuther, J. Appl. Phys. **91**, 8754 (2002).
[26] O. Thomas, Q. Shen, P. Schieffer, N. Tournerie, and B. Lepine, Phys. Rev. Lett. **90**, 017205 (2003).
[27] G. Wastlbauer and J. A. C. Bland, Adv. Phys. **54**, 137 (2005).